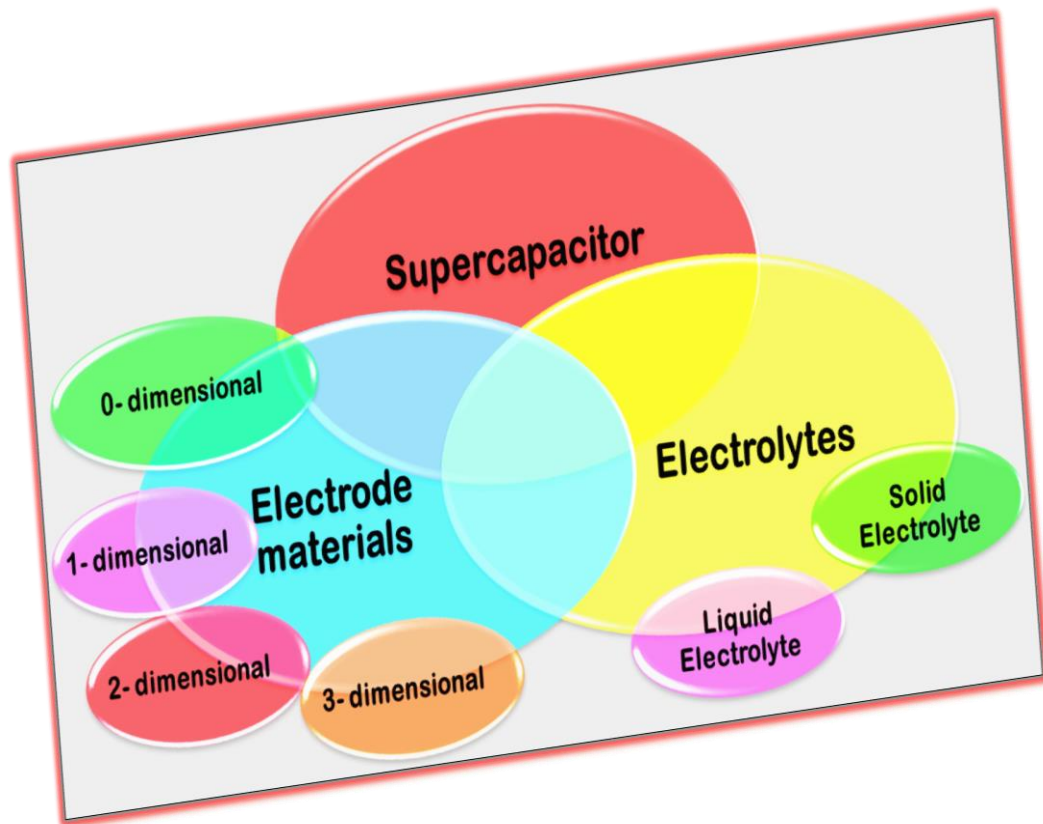


Chapter 2

Literature review



2. Literature review

2.1 History of supercapacitor

Capacitors are well known passive circuit elements, which can store electrical energy temporarily. The charge storage phenomena was first observed by Ewald Georg von Kleist of Pomerania, in a water filled hand held glass jar in the year of 1745. In 1746, Pieter van Musschenbroek, a Dutch physicist discovered a similar kind of capacitor known as Leyden jar. In the following year the Daniel Gralath improved the performance of Leyden jar by combine several jars. The improved flat capacitor design as show in the fig2.1 (a) was then proposed by Benjamin Franklin. The electrolytic capacitors having same anode and cathode materials with cell structure like batteries was the next step in the growth of capacitor devices. Before invention of supercapacitor, aluminium ceramic capacitors were the mostly used electrolytic capacitors. In aluminium electrolytic capacitors, among the two pieces of aluminium foil one was etched to form aluminium oxide's thin layer which acts as dielectric as shown the cross sectional view of the device fig 2.1 (b).

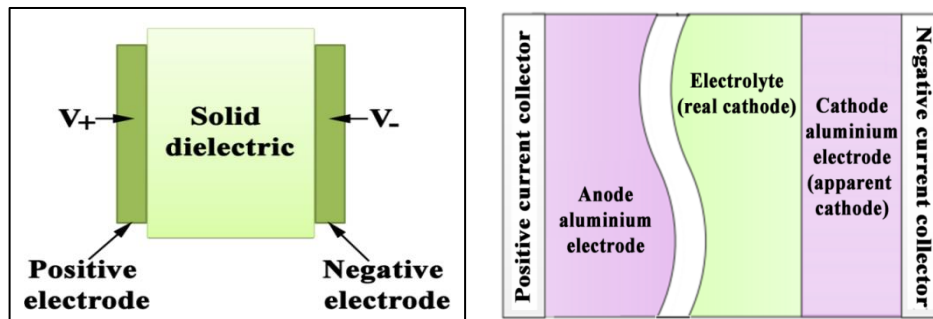


Figure.2.1 Schematic of (a) Electrostatic capacitor, (b) Aluminium electrolytic capacitors.

The electric double layer capacitor was the third generation evolution of capacitive devices. The first electric double layer capacitor was discovered in 1957 by general electric engineers, where they used porous carbon and aqueous electrolyte. At the initial stage, it was believed that energy was stored in the pores of the porous carbon although the mechanism was unknown at that time. Later, Standard Oil of Ohio's (SOHIO) used activated charcoal as electrode materials and an insulating thin separator in between to develop a new design of electrochemical capacitor, which serves as the basis design of the supercapacitor to date. They failed to commercialize it and sold the technology to

NEC which then commercialized in 1978. Tassati and Buzanca examined the performance of ruthenium oxides in the year of 1971 and observed the same electrochemical behaviour with a capacitor.^{1,2} Further, more research was carried out on the supercapacitor based on ruthenium oxide in between 1975 to 1980. Initially after its discovery, it was mainly used as a power backup in the computers and from mid-90's to date some companies such as Panasonic, NEC/TOKIN, Maxwell Technologies others invest for the development of electrochemical capacitors. From the market analysis done by Lux Research, it was observed that, the market for ECS was estimated to about \$208 million in 2009 while in 2014 it reached \$877 million and continues to increase in the recent years due to its application in cell phones, digital cameras and smart grid etc.³⁻⁵

2.2 Specific energy and specific power comparison of ECSs, batteries and fuel cells

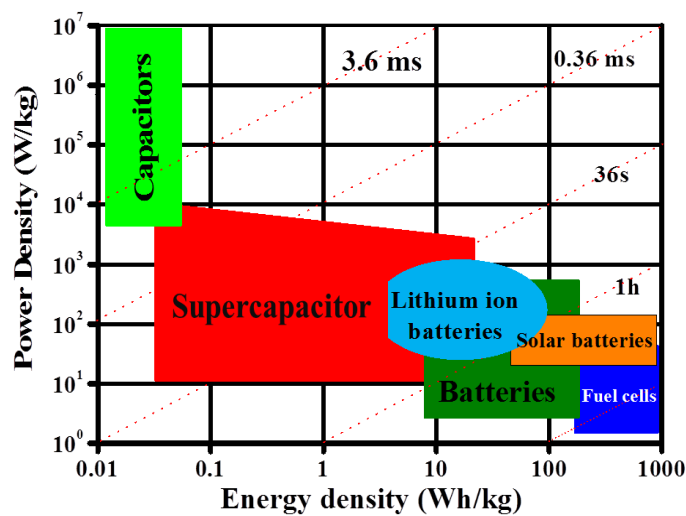


Figure 2.2 Ragone plots of different energy storage devices.

The energy storage performance of different energy storage systems can be characterised by Ragone plot as shown in the fig 2.2. The require time for charging and discharging of the various energy storage systems are represented by the dash lines. From the Ragone plot it is visualise that capacitors have greater specific power compare to fuel cells and batteries but its energy density is much lower compare to the fuel cells and batteries, which indicates that charging discharging of capacitors is very fast and produces high power but it can store low energy per unit mass or volume, whereas

batteries take large time for charging and discharging but high specific energy storage property. Supercapacitor fills the power gap between capacitors and batteries since supercapacitor have greater power density than batteries and high energy density than conventional capacitors.

2.3 Classification of Supercapacitors

Supercapacitors can be classified into three types based on their charge storage mechanism known as electrical double-layer capacitors (EDLCs), pseudocapacitors (PSCs) and hybrid capacitors(HSCs) as shown in the fig2.3.⁶ Carbon based (such as active material like Graphene, carbon aerogel, carbon nanotubes etc.) EDLC is most common used supercapacitor.^{6,7-10} The transition metal oxides (ruthenium oxide, manganese oxide, tin oxide, cobalt oxide)¹¹⁻¹⁹ transition metal dichalcogenides (TMDCs),²⁰ hydroxides ²¹⁻²³ and conductive polymer (polyaniline, polypyrrole, polythiophene). ²⁴⁻²⁷ are most commonly used electrode materials for pseudocapacitor. Low capacitance in EDLC and poor cycle's stability in pseudocapacitors confines their practical application. Innovative approaches to raise the specific capacitance, stability and energy density are to develop hybrid electrode materials for supercapacitor by adding electrochemically active materials with carbonaceous materials. This kind of SCs knows as Hybrid supercapacitors (HSCs).



Figure2.3 Schematic of Classification of Supercapacitor

2.3.1 Electric double layer mechanism

In the 19th century, von Helmholtz was first described the idea of double layers, which consist of few nanometres thick double layers of opposite charge forms between the electrode/electrolyte interface(Figure 2.4a), where energy stored due to ion adsorption. Further it was understood that ions on the electrolyte side of the double layer suffered thermal fluctuation according to the Boltzmann principle, as a result of that ions could

not remain static in the form of compact array. Later, Gouy and Chapman improved the Helmholtz double-layer model. According to the Gouy–Chapman a diffuse layer is formed due to the thermal fluctuation of the electrolyte ions as shown in the figure 2.4(b). In the Gouy–Chapman model ions were considered as point charges. Combining Helmholtz model with Gouy–Chapman model, Stern presented a model, which describe compact and diffusion region explicitly. The compact layer made of by inner Helmholtz plane (IHP), which is the distance of closest approach of adsorbed ions and outer Helmholtz plane (OHP) refers the plane where the diffusion layer start. According to the Stern model capacitance of the EDLC is the series combination of stern layer capacitance and diffusion layer capacitance as shown in the figure 2.4(c).

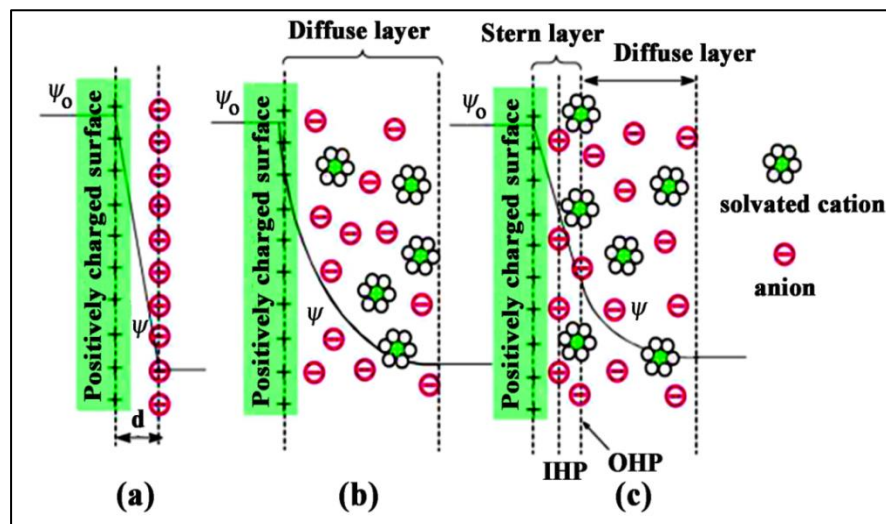


Figure 2.4 Schematic of mechanism of electric double layer capacitor.

2.3.2 Pseudocapacitance mechanism

In case of pseudocapacitor a fast reversible Faradaic (redox) reactions takes place on the electrode in presence of external potential. B.E. Conway in 1970 was first discussed there are mainly three faradic mechanisms process involves in pseudocapacitive behaviour: (1) under potential deposition, (2) redox pseudocapacitance and (3) intercalation pseudocapacitance as shown in the fig 2.5. Langmuir type electroporation of H on the noble metal substrate is an example of under potential deposition, where adsorbed monolayer of the metal ions obtain on the different metal substrate at well above their redox potential. The ions are electrochemically adsorbed onto active material's surface in case of redox pseudocapacitance, whereas ion intercalation into sheets of an active material without any crystallographic phase change terms as intercalation pseudocapacitance.

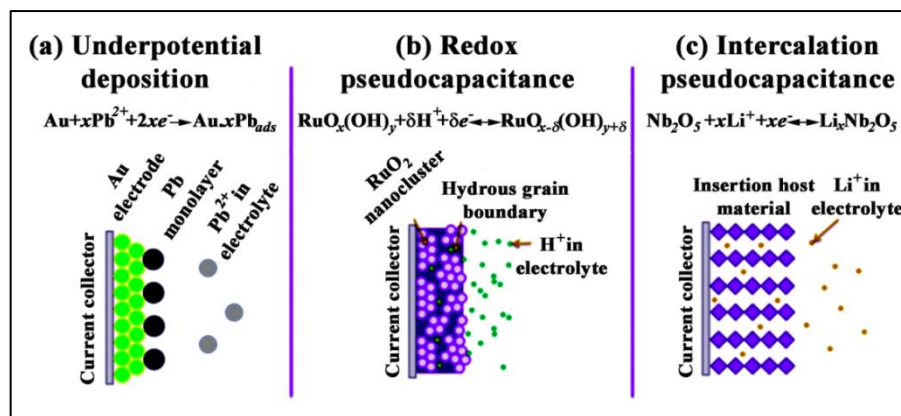


Figure 2.5 Schematic of mechanism of pseudocapacitors

2.4 Supercapacitor material selection

Energy density of the supercapacitor is directly proportional to the square of the voltage window as well as the capacitance value, so enhancement of the energy density can be done by increasing both voltage window and capacitance value. Notably, the electrode material's structure and morphology and electrolyte's composition is closely linked with both of voltage window as well as capacitance.

2.4.1 Electrode materials for Supercapacitor

Specific capacitance, energy density, power density and stability are the key performance parameters of supercapacitors and these parameters are directly depends on the electrode materials. An ideal electrode material should have the following properties:

- High specific surface area.
- Extra electroactive sites.
- Porous structure.
- High electronic conductivity.
- High thermal and chemical stability.
- Low cost of raw materials.

Nanostructures of the electrode materials also play an importance role to achieve the aforementioned factors. Different nanostructures material can be categorised into zero dimension (0-D), one dimensional (1-D), two dimensional (2-D) and three dimension (3-D) respectively.²⁸ Spherical or nearly spherical nanoparticles with an aspect ratio close to 1 are fall under the 0-D category and quantum dots, nanoparticles, nanosphere etc. are belongs from these category. Fiber like shaped nanomaterial with high aspect ratio such as nanotubes, nanowires, nanofibers, nanopillars, nanobelts etc. are

considered as 1-D. One or few atomic layer nanomaterial's with higher bond strength than three dimensions are defined as two dimensional (2-D) nanomaterial. They include Graphene, Graphene oxides, and other layered materials such as MoS₂, VS₂, MoO₃, VOPO₄ etc. Carbon nanofoams, 3-D porous carbon and Graphene aerogel are regarded as three dimensional (3-D) electrode materials for supercapacitors.

2.4.1.1 Zero dimensional nanomaterials (0-D)

Nanomaterials with three dimensions constrained on nanoscale are defined as 0-D nanomaterials which have three subclasses solid zero dimensional, hollow zero dimensional and core-shell zero dimensional nanostructures. In this type of materials electrons are confined in all three directions.

2.4.1.1.a. Solid 0-D nanostructures

Among different nanostructures, solid 0-D nanostructures such as ACs, carbon nanospheres, transition metal oxides (e.g. RuO₂²⁹, NiO^{30, 31, 32}, Fe₃O₄³³, MnO₂³⁴) are generally used as electrode materials for supercapacitor. Chemically or physically synthesized activated carbon from various carbonaceous precursors like coal, wood etc. are one of the most commonly used carbon based materials in supercapacitor because ACs provides greater specific surface area even up to 3000 m²/g.³⁵ Though ACs have high surface area, the obtained specific capacitance of ACs based supercapacitors are quiet small (<10μF/cm²), because specific capacitance is also depends on the distributions of pore sizes, electronic conductivity and electrolyte's accessibility too. Gogotsi, Simon et.al reported carbon onion having surface area 500 m²/g showed better electrochemical performance than ACs. This is due the fact that for onion like structure, surface is fully open to the electrolyte ions.^{36,37} The above mention criteria are also applicable for pseudocapacitive materials such as TMOs, TMDCs etc. Conducting nano porous gold/MnO₂ hybrid exhibited specific capacitance of 1145 F/g at 50mV/s, because nano porous gold provides an easy path to access the electrons and ions.³⁸ K. J. Stevenson and co-worker reported, LaMnO₃ nanoparticles based supercapacitor, which obtained 610 F/g capacitance at scan rate of 2 mV/s. For perovskite-type materials also store charge through oxygen intercalation.³⁹ Hence, besides the activated carbon and TMOs, perovskite materials are the new candidate for supercapacitor applications.

2.4.1.1.b. Hollow 0-D nanostructures

The properties like short transportation path of charge, low density and high surface to volume ratio of hollow 0-D materials make them attractive candidates for

supercapacitor application. For the synthesis of hollow 0-D materials, there are three different procedures such as template-free, soft templating and hard templating. The controlled shape, size and structure of 0-D nanomaterials can easily achieved by hard templating methods rather than the other two as mention above. Hollow carbon nanosphere obtained by hard templating method delivered large specific surface area up to $1704 \text{ m}^2/\text{g}$ and $1.6 \text{ cm}^3/\text{g}$ pore volume with $\sim 6.4 \text{ nm}$ pore width. The hollow carbon nano sphere based supercapacitor exhibits 251 F/g specific capacitance value at 50 mV/s scan rate.⁴⁰ Furthermore, multiple shelled hollow 0-D structure of the nano materials such as Fe_2O_3 , MnO_2 , NiO , and Co_3O_4 has been studied as well.⁴¹⁻⁴⁷ Zhang et.al was reported Single, double, and triple shelled NiO nanospheres. Among them double layer NiO nanospheres exhibits $92.00 \text{ m}^2/\text{g}$ surface area with 612.5 F/g specific capacitance.⁴⁸

2.4.1.1.c. Core-shell 0D nanostructures

The thin shell coated hollow or solid nano particle is known as core-shell 0-D nano structure. A core-shell nano structure prepared by combining carbonises and faradic materials show good mechanical and chemical stability, least agglomeration and improved electrical conductivity.⁴⁹⁻⁵¹ Zhao et.al reported hollow carbon sphere/polyaniline (PANI) core-shell structure exhibits 525 F/g specific capacitance, whereas that for hollow carbon sphere is only 268 F/g .⁵²With increasing amount of PANI, electrochemical performance of the electrode materials becomes poor; this is due to the fact that with increasing PANI pores will be blocked and reduced accessibility of ions. Zhao and co-worker have grown MnO_2 shell on carbon core as supercapacitor electrode materials by direct redox reaction at 70°C using hollow spheres of graphitic carbon and potassium permanganate solution. The hybrid core-shell structures with 64 wt\% MnO_2 displayed 190 F/g specific capacitance at 0.1 A/g .⁵⁰

2.4.1.2 One dimensional nanomaterials (1-D)

Fiber shaped nanomaterials with high aspect ratio is categorised as 1-D nano-structures. Nanotube, nano fibres, nano wire, nano pillar, nano rods etc. fall into that category. 1-D nano-structures have good chemical and physical properties. 1-D nano-structures also provide decent electrical transport properties to increase the kinetics of the electrochemical reactions. Due to the above mentioned properties 1-D nano-structures have been widely examined for the electrode materials for supercapacitors. Homostructures and heterostructures are two main categories of 1D nanostructure.

2.4.1.2.a 1-D Homostructures

1-D homostructures can be defined as a structure which contains only one particular structure like nanorods, nanotubes, nanofibers etc. 1-D homostructures can be classified into three groups such as nanotubes, nanorods/nanopillars and nanowires.

Nanorods/nanopillars having aspect ratios less than 10, which confine the improvement of surface area of the nanorods compared to nanowires. Thomas and co-workers have synthesized highly ordered carbon nanopillars of diameter and length 95 nm and 200 nm respectively prepared by simple, rapid and cost-effective spin-on nano imprinting technique. The highly ordered carbon nanopillars electrode exhibits specific capacitance of 3.4 mF/cm^2 .⁵³ Tong et al. reported oxygen deficient Fe_2O_3 nanorods based supercapacitor, which obtained 64.5 F/g specific capacitance.⁵⁴

High aspect ratio (>10) of nanowires not only enhance the charge transportation path also offer large surface area on to which charges are stored, and due to that reason we get enriched electrochemical performance. The vertically aligned PANI nanowires based electrochemical capacitor showed 1142 F/g specific capacitance at a current density of 5 A/g .⁵⁵ Horng and co-workers have successfully synthesized PANI nanowires on Carbon cloth, which delivered highest specific capacitance of 1079 F/g , at 1.73 A/g with 86% capacitive retention after 2100 cycles.⁵⁶ Recently, ternary metallic oxides have attracted significant attention as electrode materials due to their multiple oxide states. Lou et al. reported NiCo_2O_4 nanoneedle electrode supercapacitor showed 1118.6 F/g specific capacitance.⁵⁷ Nanotubes offer greater specific surface area per unit mass than solid nanowires or nanofibers because of their hollow interior structure. As a result specific capacitance also enhanced with compare to the solid 1-D nano structures. Xai and co-worker have compared the performance of MnO_2 nanotube and MnO_2 nanowire as electrode material.⁵⁸ The MnO_2 nanotube and MnO_2 nanowire obtained a specific capacitance of 320 F/g , and 101 F/g respectively. Chi Chang Hu and co-worker have successfully synthesized RuO_2 nanotube array by deposition technique which exhibited 550 F/g specific capacitance.⁵⁹ Carbon nano tubes are one of the most used 1-D nano materials for supercapacitor electrode application because its provides high electronic conductivity, decent thermal and mechanical stability, high specific surface area and porosity. H. Pan and his group reported pure CNT based electrode obtained highest specific capacitance of 100 F/g .⁶⁰

2.4.1.2.b 1-D Heterostructures

Recently, 1-D heterostructures having more than one component considered as one of the probable candidates for supercapacitor electrode because synergic enhancement of properties such as electrical conductivity, ionic transport, mechanical stability and electrochemical reversibility after heterostructures formation. 1-D core-shell heterostructures provides enhanced cycles stability and better electrochemical performance than other heterostructures due their exclusive structural properties that reduced the aggregation chance of the active materials as well as overcome the side reaction problem between active materials and electrolyte. P.L.Taberna et.al reported Cu/Fe₃O₄ core shell nanostructure. There are several core shell nanostructure such as Au/MnO₂, Ni/MnO₂, Ni/Co₃O₄, Mn/MnO₂, AuPd/MnO₂, CuO/AuPd/MnO₂, Ni/NiO have been already reported as supercapacitor electrodes.²⁸ Zhai and co-workers reported CNT/PPy–MnO₂ core shell nano structure based supercapacitor which delivered specific capacitance of 268 F/g.⁶¹ CNT/MnO₂ core shell based supercapacitor showed two times higher specific capacitance than MnO₂. Fan's group has reported several with 1D core–shell heterostructures such as Co₃O₄/NiO, Co₃O₄/MnO₂, Co₃O₄/PEDOT//MnO₂CoO/NiHON, CoO/TiO₂. The Co₃O₄/MnO₂ core–shell heterostructures delivered specific capacitance of 480 F/g at 2.67 A/g. Due to improved electronic conductivity of NiCo₂O₄ than Co₃O₄ Liu's group used NiCo₂O₄ instead of Co₃O₄. The NiCo₂O₄/Ni_xCo_{1-x}(OH)₂ core–shell has obtained specific capacitance up to 1500 F/g with 67% retention. Similarly, Co₃O₄@PANI, V₂O₅@PPy, V₂O₅@PEDOT–MnO₂, MnO₂@PEDOT–PSS, MnO₂@PPy have been shows better electrochemical performance than metal oxides like MnO₂, V₂O₅, Co₃O₄ because core shell structures prevent the dissolution problems after cycling.^{62,28} The protecting coating thickness and electrochemical performance are related to each other, protecting coating can prevent the dissolution issues but with the increasing thickness accessibility of ions also decreases. So, further study should need to resolve this problem.

2.4.1.3 Two dimensional nanomaterials (2-D)

The sheets or flakes like nanostructure with high aspect ratio are defined as two dimensional nanostructures. 2-D materials exhibited large specific surface area, mechanical and chemical stability, excellent electrical conductivity, due to those unique properties 2-D materials becomes promising candidates for supercapacitor application. In the 2-D nanostructure greater contact area with the electrolytes for utilization of active materials also plays an anchoring role to enhance the electrochemical

performance. Like 1-D nanostructure, 2-D nanostructures also have two main categories, named as homostructures and heterostructures.

2.4.1.3.a 2-D Homostructures

The 2-D homostructured electrode materials can be classified into three main subcategories as following

- (1) Graphene as active materials for EDLC.
- (2) Transition metal oxides and hydroxides as active material for pseudocapacitor.
- (3) Transition metal dichalcogenides (TMDs) and transition metal carbides and/or nitrides (MXenes).

2.4.1.3.a (i) Graphene

Among the different forms of carbon, 2-D graphene have been broadly used electrode materials of supercapacitors. In the year of 2004, monolayer of sp^2 bonded carbon atoms in a 2-D honeycomb lattice (Graphene) was experimentally discovered by K.S. Novoselvo and co-workers.⁶³ Now a day, Graphene is one of the most common active materials in field of energy storage its provides larger theoretical specific surface area ($2630 \text{ m}^2/\text{g}$), high mechanical and chemical strength and extremely high electronic conductivity.⁶⁴ However, restacking properties of graphene sheets plays a negative role due to which graphene based supercapacitors does not provides expected results. The theoretical value of the graphene based supercapacitor is 550 F/g whereas reported values are in the range from 80 to 118 F/g .⁶⁵ Due to the hydrophilic nature of the chemically synthesized reduced graphene oxides (rGO) for presence of functional groups on rGO the production of composites with metal oxides becomes much easier. Further modification can also be done by adding other functional groups on rGO, which serve as the redox centres. Ruoff et al. have produced chemically modified graphene (CMG) with a specific surface area $705 \text{ m}^2/\text{g}$. The resulting CMG based supercapacitor showed specific capacitance of 135 F/g in aqueous electrolyte and that 99 F/g in presence of organic electrolyte.⁶⁵ Ruoff and co-workers reported the synthesis the activated rGO using KOH in GO with a specific surface area of $3100 \text{ m}^2/\text{g}$. The resulting activated graphene delivered high specific capacitance of 166 F/g at a current density of 5.7 A/g and $\sim 97\%$ of the capacitance retention after 10000 cycles.⁶⁴ Vacuum low-temperature exfoliated graphene based supercapacitor showed specific capacitance of 220 F/g and 120 F/g in presence of aqueous and organic electrolytes respectively.⁶⁶ The rGO prepared by thermal treatment at 200°C from GO also delivered a specific capacitance of 122 F/g at 5 mA .⁶⁷ El-Kady et al. reported laser-treated well aligned laser-scribed

graphene (LSG) obtained using a standard Light Scribe CD/DVD optical drive. Cross sectional The supercapacitor based on the LSG sheets delivered enhanced electrochemical performance than the other graphene-based flexible supercapacitors.⁶⁸

2.4.1.3.a (ii) Metal oxides and hydroxides

2-D transition metal oxides such as MnO₂, RuO₂, MoO₃, NiO, V₂O₅, Co₂O₃, IrO₂, and SnO₂ are played an important role to development of hybrid supercapacitors. Table 1 shows the theoretical specific capacitance of some transition metal oxides. Though, the practical specific capacitances of those metal oxides are far behind the theoretical value due to the low electrical conductivity. Kang and co-workers reported 2D MnO₂ prepared by soft template technique, exhibited a high specific capacitance of 774 F/g.⁶⁹ RuO₂ thin films supercapacitor delivered specific capacitance up to 730 F/g.⁷⁰

2.4.1.3.a (iii) Transition metal dichalcogenides (TMDs)

Recently, layered TMDS like MoS₂, TiS₂, WS₂, and VS₂ have taken attention due to their prospective applications such as sensor, opto-electronics and electrode of SC. The shortcomings of graphene could easily overcome due to the unique properties of TMDs. Among TMDS, MoS₂ have taken the most attention than other because of its intrinsic conductivity and predicted greater theoretical capacity than graphene.^{71,72} Edge-oriented MoS₂ films micro-supercapacitor reported by Soon and co-workers showed CNT electrodes like electrochemical performance.^{73,74} Geng and co-workers reported flower-like MoS₂ electrode material exhibited a specific capacitance of 168 F/g with 93% capacitance retention after 3000 cycles. Feng and co-worker reported in plane supercapacitor by layered VS₂, which was exhibited specific capacitance of 4760 $\mu\text{F}/\text{cm}^2$ with 90 % capacitance retention after 1000 cycles.⁷⁵

2.4.1.3.a (iv) Transition metal carbides and/or nitrides (MXenes) nanostructure

A new promising candidate for supercapacitors consisting highly 2-D conductive carbide and carbonitride layers with a hydrophilic, primarily hydroxyl-terminated surface labelled as MXenes was recently introduced by Gogotsi and his team. MXenes based supercapacitor offered high capacitance (300 F/cm³) more than that of porous carbon, due to the cations (Li⁺, Mg²⁺, Al³⁺, Cs⁺, K⁺, NH⁴⁺, Na⁺, Ba²⁺, Ca²⁺) intercalation.^{76,77} 2-D MXenes are derived from layered hexagonal carbides or carbonitrides (MAX phases) by removing A layers from it. In the formula of M_{n+1}AX_n (n = 1, 2, 3), M signifies an early transition metals (e.g. Ti, V, Cr, Nb, etc.), A represents IIIA or IVA elements (e.g. Ga, Al, Si, Sn, In or Ge); and X represents C and/or N. Till now, only eleven MXenes are tested experimentally though variety of

MXenes predicted theoretically.^{78,79} Lukatskaya and co-worker reported $\text{Ti}_3\text{C}_2\text{T}_x$ MXene material based supercapacitor which showed 350 F/cm^3 volumetric capacitance in presence of aqueous NaOH electrolyte.⁷⁶

2.4.1.3.b 2-D heterostructures

The electrochemical performances of the 2-D homostructures is enhanced after formation of 2-D heterostructures, these is due to the fact that the electrical conductivity, thermal stability and mechanical strength of the composites or hybrid electrode materials are improved than 2-D homostructures.

2.4.1.3.b (i) Graphene/metal oxides and hydroxides hybrids or nanocomposites

Graphene have potential application as an electrode material of EDLC. The Graphene/TMOs and Graphene/hydroxides hybrids offer both pseudo capacitance and EDLC contribution, which enriched the performance of supercapacitor. RuO_2 /graphene hybrid containing 30 wt% graphene sheets exhibited specific capacitance of 370 F/g at 2mV/s.⁸⁰ Zhang and co-worker reported rGO/ RuO_2 hybrid delivered maximum specific capacitance of 357 F/g at a current density of 0.3 A/g.⁸¹ Graphene/ MnO_2 hybrid synthesized by microwave irradiation offered specific capacitance of 310 F/g at 2 mV/s with 95 % capacitance retention after 15000 cycles test.⁸² Dong et.al reported Co–Al hydroxide nanosheets/graphene based supercapacitor delivered 880 F/g specific capacitance at 5 mV/s with 99% capacitance retention after 2000 cycles.⁸³ Ni(OH)₂ nanosheet/ Graphene exhibited specific capacitance of 660.8 F/cm^3 , which also offered 98.2% capacitance retention after 2000 cycles.⁸⁴ Other metal oxides (such as ZnO, Fe_3O_4 , SnO_2) hybrids with graphene also offered improved performance.⁸⁵⁻⁸⁷

2.4.1.3.b (ii) Graphene-dichalcogenides

Like TMOs, layered TMDs also used widely in the field of energy conversion and energy storage due to its decent electrocatalytic performance, high chemical stability, low cost. Besides of that, layered structure of the TMDs also helpful for the insert and remove of electrolyte ions. But the poor cycle stability and low conductivity limits its practical application in the energy storage field. Graphene/TMDs hybrids are offers improved electrochemical performance with good chemical stability and enriched conductivity due to graphene addition. Rout and co-worker reported hydrothermally synthesized WS_2 /rGO hybrid electrode material, which exhibited specific capacitance of 350 F/g at 2 millivolt per sec scan rate.⁸⁸ E.G.da Silveira and his team investigated the electrochemical performance of MoS_2 /rGO hybrid. The hybrid exhibited 265 F/g

specific capacitance at 10 mV/sec scan rate and 92% capacitance retention after 1000 cycles.⁸⁹

2.4.1.3.b (iii) Graphene /2D transition metal carbides and vanadyl phosphate

Zhao and co-worker investigated the electrochemical properties of 2-D Titanium carbide ($\text{Ti}_3\text{C}_2\text{T}_x$)/rGO composites, with different wt% of rGO. The obtained maximum specific capacitance was 154.3 F/g at 2A/g with 85% capacitance retention after 6000 cycles. Gogotsi et.al reported free standing $\text{Ti}_3\text{C}_2\text{T}_x$ /rGO electrode, which revealed a volumetric capacitance of 1040 F/cm³ at 2 mV/s scan rate. Layered VOPO₄/graphene hybrid based flexible supercapacitor exhibited areal capacitance of 8360.5 mF/cm² and 96% capacitance retention after 2000 cycles⁹⁰

2.4.1.4 Three dimensional nanomaterials (3-D)

3-D nanomaterials are made of low dimensional building block. Carbon nanofoams or sponges and nickel foam are serving as extremely porous and conductive templates on which metal oxides, polymers, graphene; CNTs can be deposited to form 3D nanostructures for supercapacitor electrode. 3-D nanomaterials provides large specific surface and well defined path to access electrolyte ions due to its porous structure.⁹¹⁻⁹⁶

Xie and co-worker reported MnO₂-coated 3D grapheme exhibits specific capacitance of 130 F/g and showed 82% capacitance retention after 5000 cycles.⁹⁷ The asymmetric supercapacitor fabricated by Ni_{0.61}Co_{0.39} oxide on nickel foam exhibited a specific capacitance of 1523 F/g at 2 A/g current density, where the used electrode acted.as a positive electrode with activated carbon as a negative electrode. The asymmetric supercapacitor also obtained high energy density of 36.46 W h/ kg at a power density 142 W/kg and 95% capacitance retention after 1000 cycles.⁹⁸ Zhou and co-worker reported CoO-PPy on 3D nickel foam based supercapacitor, which showed specific capacitance of 2223 F/ g at 1 mA/cm².⁹⁹

2.4.1.5 Advantages of 2-D materials

Among different nanostructures, two dimensional nano materials become attractive electrode materials to achieve the flexible supercapacitors. And this is due to their unique properties such as

- a. 2-D nanomaterials provide large specific surface area.
- b. It provides macro mechanical flexibility to form thin films.
- c. Atomically thick layer 2-D materials have high electrochemical active sites.
- d. Moreover, 2-D materials possess confined thickness, which provide well-behaved electrical properties also.

2.4.2 Electrolyte for Supercapacitor

The electrolyte also played an important role for the development of ECs. Electrolytes are one of the important components of SCs, providing ionic conductivity. The performance of electrochemical capacitor is directly influenced by the size and nature of the electrolyte ions, concentration of ions, electrolyte/electrode materials interaction and electrochemical stable potential window (ESPW) of the electrolytes. During the past several decades, various types of electrolytes have been already introduced and each electrolyte has its own advantages and drawbacks. The electrolytes are classified as: (a) Liquid electrolytes, (b) Solid state / quasi-solid state electrolytes and as shown in the figure 2.6.

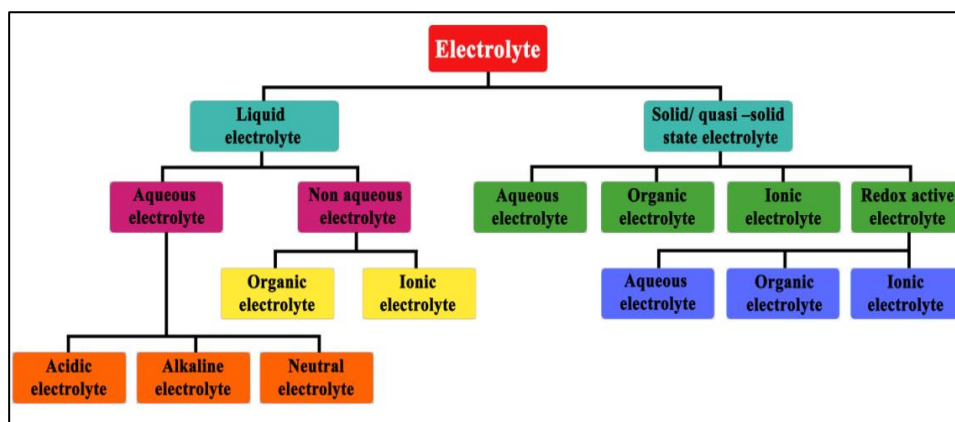


Figure 2.6 Types of electrolytes for supercapacitors.

2.4.2.1 Liquid electrolytes

Liquid electrolytes can be broadly divided into three main sub grouped named as (i) aqueous electrolytes,(ii) organic electrolytes and (iii) ionic electrolytes. Aqueous electrolytes provide high conductivity but low electrochemical stable potential window (ESPW) whereas organic and ionic electrolytes possess high ESPW but struggle with low ionic conductivity. In addition, potential leakage problem of the liquid electrolytes can be resolved by replacing it with solid electrolyte, but they also suffer from low ionic conductivity.

2.4.2.1 a. Aqueous electrolytes

For the improvement of energy density of supercapacitors, aqueous electrolytes are poor choice due to its low potential window. However, aqueous electrolytes have been used widely in research because of its low cost and easily handled nature than organic and ionic electrolytes. Besides of that aqueous electrolytes also offered high conductivity than other liquid electrolytes, which is beneficial to enhance power

delivery and dropping the equivalent series resistance (ESR) of ECSs. The ionic conductivity of the different aqueous electrolytes are shown in the table (2.1).¹⁰⁰⁻¹⁰⁴

Table 2.1 Ionic conductivity, sizes of the bare and hydrated cations and anions of ions

Ion	Bare ion size (Å)	Hydrated ion size(Å)	Ionic Conductivity (S cm ² mol ⁻¹)
H ⁺	1.15	2.80	350.1
K ⁺	1.33	3.31	73.5
Li ⁺	0.60	3.82	38.69
Mg ²⁺	0.72	4.28	106.12
Na ⁺	0.95	3.58	50.11
Ca ²⁺	1.00	4.12	119
SO ₄ ²⁻	2.90	3.79	160.0
OH ⁻	1.76	3.00	198
Cl ⁻	1.35	4.04	127.8
PO ₄ ³⁻	2.23	3.39	207
CO ₃ ²⁻	2.66	3.94	138.6

There are mainly three types of aqueous electrolytes named as acidic aqueous electrolytes, alkaline aqueous electrolytes and neutral aqueous electrolytes. 1M H₂SO₄ electrolyte with ionic conductivity 0.8 S cm⁻¹ at room temperature is most frequently used acidic electrolyte.¹⁰⁵The acidic aqueous electrolytes widely used for EDLCs. Besides of acidic electrolytes, KOH, NaOH and LiOH etc. have also been studied as alkaline aqueous electrolytes and among them 6M KOH has exhibited maximum ionic conductivity (0.6 S/cm at 25°C). These alkaline electrolytes can be used for all three types of electrode materials. It can be reported that maximum limiting voltage is 1.3V for both acidic and alkaline electrolytes, independent on the nature of the electrode materials used for ECSs, whereas reported maximum cell voltage is 2.2 V for the neutral electrolyte.^{106,107} LiCl, Li₂SO₄, Na₂SO₄, NaCl, K₂SO₄, KCl, MgSO₄ etc. are previously reported neutral electrolyte, which are generally used in pseudocapacitors () and hybrid capacitors(HSCs). Among different neutral electrolytes Na₂SO₄ is frequently used for PSCs. Some previously reported aqueous electrolyte-based ECSs and their performance are shown in the table.

Table 2.2 Table of previously reported aqueous electrolyte-based ECSs and their performance

Aqueous Electrolyte	Electrode materials	Specific capacitance (F/g)	Energy density (Wh/kg)	Power density (W/kg)	Ref.
Strong acid electrolyte:					
1M H ₂ SO ₄	Graphene/mPANI	749 at 0.5 A/g	11.3	106.7	108
1 M H ₂ SO ₄	AC fibers	280 at 0.5 A/g			109
2 M H ₂ SO ₄	carbon nanofiber networks	204.9 at 1 A/g	7.76	~100	110
0.5M H ₂ SO ₄	RuO ₂ -graphene	479 at 0.25 A/g	20.28	600	111
1 M H ₂ SO ₄	PANI-grafted rGO	1045.51 at 0.2 A/g	8.3	60000	112
Strong alkaline electrolyte:					
2 M KOH	sub-3 nm Co ₃ O ₄ Nanofilms	1400 at 1 A/g	-	-	113
1 M LiOH	MnO ₂ nanoflower	363 at 2mV/s	-	-	114
6 M KOH	highly porous graphene planes	303 at 0.5 A/g	-	-	115
6 M KOH	p-CNTn/CGBs	202 at 0.325 A/g	4.9	150	116
Neutral electrolyte:					
0.5 M Na ₂ SO ₄	seaweed carbons	123 at 0.2 A/g	10.8	-	117
1M NaNO ₃	AC	116 at 2mV/s	-	-	118
4 M NaNO ₃ -EG	AC	22.3 at 2 mV/s	14-16	~500	119
1 M KCl	MnCl ₂ -doped PANI/SWCNT	546 at 0.5 A/g	194.13	550	118
1M Na ₂ SO ₃	well-ordered mesoporous carbon/Fe ₂ O ₃	235 at 0.5 A/g	39.4	-	119

2.4.2.1 b. Non-aqueous electrolytes

The non-aqueous organic and ionic electrolytes were employed to overcome the potential barrier (up to 3.5 V) over the aqueous electrolyte. The higher operation cell potential can provide an improved energy and power densities. Triethylmethylammonium tetrafluoroborate and tetraethylammonium tetrafluoroborate in acetonitrile are mostly used organic electrolyte, which provides a comparatively larger potential window around 2-2.5 V. Organic electrolytes have a larger cost, lower conductivity and also requires complicated purification before use. It has been already reported that the electrochemical performance of activated carbon is poorer in organic electrolytes (50-150 F/g) than in aqueous electrolytes (100-300 F/g).^{120,121} This is due the fact that, effective ions size of the electrolyte in organic solutions is much larger than those in water. Moreover, the disadvantages like electrolyte depletion upon charge and safety concerns related to the toxicity, instability also bound the use of organic electrolytes. Some previously reported organic electrolytes performances are shown in the table 2.3. Ionic liquids, a type of organic salts (molten salts) have many potential advantages like wide ESPW, high thermal, chemical and electrochemical stability; non-flammability. Additionally, depending on the requirements of electrochemical performances like operating cell voltage, working temperature etc. compositions of the electrolytes can also be optimized or customized due to its highly tunable physical and chemical properties. Low ionic conductivity at room temperature, high viscosity limits its application, so ionic liquids are mainly used at high temperature. Ionic liquids are completely composed of cations and anions. Tetrafluoroborate (BF_4^-), hexafluorophosphate (PF_6^-) bis (trifluoromethanesulfonyl) imide (TFSI⁻), bis(fluorosulfonyl)imide (FSI⁻), and dicyanamide (DCA^-) are the commonly used anions of ILs whereas imidazolium, pyrrolidinium, ammonium, sulfonium, phosphonium commonly used cations. Balducci and co-worker reported N-butyl-N-methylpyrrolidinium bis(trifluoromethanesulfonyl)imide ionic liquid filled AC supercapacitor, which delivered a C_{sp} of 60 F/g with high cycling stability for 40000 cycles. G. Yushin and co-worker reported polypyrrole-derived activated carbon based symmetric EDLC with EMImBF₄ ionic liquid electrolyte showed a specific capacitance of 300 F/g. Among the several ILs, [EMIM][BF₄] electrolyte have higher conductivity (14 mS/cm at 25°C). But it is much lower than TEABF₄/CAN (59.9 mS/cm at 25°C) organic electrolyte. The improvement of ionic liquid for ES applications is still in the initial stage and progress is required to ensure their full utilization.

Table 2.3 Table of previously reported organic electrolyte-based ECSs and their performance

Electrolyte	Electrode materials	Specific capacitance (F/g)	Energy density (Wh/kg)	Power density (W/k)	Ref.
1 M TEABF 4 /ACN	highly porous interconnected carbon nanosheets	120–150 at 1 mV s ⁻¹	25	25000–27000	120
1 M TEABF 4 /HFIP	AC	110 at 1 mV s ⁻¹	-	-	121
0.7 M TEABF 4 /ADN	AC	25 at 20 mV s ⁻¹	~28		122
1 M TEABF 4 /PC	graphene–CNT composites	110 at 1 A g ⁻¹	34.3	400	123
MC-PC-EA	Microporous carbide derived carbon	120 at 1 mV s ⁻¹	40	90	124
0.5 M Bu 4 NBF 4 /ACN	H-carbazol-9-yl acetic acid)/TiO ₂ nanoparticles composite	462.88 at 2.5 mA cm ⁻²	89.98	-	125
1.5 M TEMABF 4 /PC	mesophase carbon microbeads/graphitized carbon	363 at 2mV /s	60	~30	112
1 M LiTFSI/ACN	MnO ₂ nanorodes–rGO//V ₂ O ₅ NWs–rGO	36.9	15.4	436.5	126
1 M LiPF 6 /EC-DM C(1:1)	Commercial AC (MSP-20)//mesoporous Nb ₂ O ₅ – carbon nanocomposite	202 at 0.325 A/ g	74	~100	127
1 M LiPF 6 /(EC-DEC 1:1):	Nanoporous Co ₃ O ₄ – graphene composites	123 at 0.2 A/g	-	-	128

2.4.2.2 Solid- or quasi-solid-state electrolytes

Now a days, solid-state or quasi solid state electrolyte based supercapacitors take tremendous attention to develop the flexible portable devices. The solid-state electrolytes plays dual role in flexible supercapacitors such as ionic conducting media and the electrode separators due to which, leakage free flexible device can easily achieved. The performance of flexible supercapacitors depends on a solid state electrolyte that shows good mechanical and chemical stability with high ionic conductivity. Generally, gel electrolyte are composed of polymer, such as polyvinyl alcohol (PVA), polyvinylpyrrolidone (PVP), polyethylene glycol (PEO) and polypolyacrylate (PAA) etc. with a proton conducting aqueous solutions. Table 2.4 presents the typical solid state electrolyte-based ECS's performance.

Table 2.4 Ionic conductivity of solid state electrolyte

Electrolyte	Type of electrolyte	Ionic conductivity (S cm ² mol ⁻¹)	Ref.
PVA/H ₂ SO ₄	Aqueous	30	129
PVA/KOH	Aqueous	0.1	130
PAM/LiCl	Aqueous	10	131
PAA/TEAOH	Aqueous	0.9	132
PVA/GO doped KOH	Aqueous	200	133
PEO/LiCO ₄ -TiO ₂ -Al ₂ O ₃	Organic	0.03	134
PEO/PC-NaTFSI	Organic	0.54	135
PVDF-HFP/PC-Mg(ClO ₄) ₂	Organic	5.4	136
PAN-b-PEG-b-PAN/LiClO ₄	Organic	11	137
PVA/BMIMCl-LiClO ₄	Ionic	37	138
PEO/EMIHSO ₄ -MIHSO ₄	Ionic	1.7	139
PEO/EMIHSO ₄ -ImHSO ₄	Ionic	2.5	139
PEGDA/EMIMTFSI	Ionic	9.4	140
PHEMA-chitosan/EMIMCl	Ionic	25	141
PVA/p-Benzenediol(PB) doped H ₂ SO ₄	Redox active aqueous	34.8	142
PVA/BAAS doped H ₂ SO ₄	Redox active aqueous	21.4	143
PVA/AQQS doped H ₂ SO ₄	Redox active aqueous	28.5	144
PMMA/PC-Fc doped TEABF ₄	Redox active organic	1.89	145
PMMA/PC 4-oxo TEMPO doped TEABF ₄	Redox active organic	1.73	145
PVA/EMIMBF ₄ doped H ₃ PO ₄	Redox active ionic	39.3	143

2.5. References

1. Wikipedia, Wikipedia, http://en.wikipedia.org/wiki/Electric_double-layer_capacitor
2. B.E Conway, *Electrochemical Supercapacitors: Scientific Fundamentals and Technological Applications*, Kluwer academic/ Plenum publishers, 1999, pp17-556
3. J. Garthwaite, "Supercapacitor Market to Surge to \$877M by 2014", <http://earth2tech.com/2009/06/10/supercapacitor-market-to-surge-to-877m-by-2014/>.
4. L. Sibley, "Researchers See Spike in Supercapacitor Demand", Cleantech Group, 2009, <http://cleantech.com/news/4576/researchers-see-spike-in-supercapacitor-demand>
5. Nano Markets, "Market for Battery and Supercapacitor Storage Systems for Smart Grid Applications Expect to reach \$8.3 Billion in 2016", <http://www.azonano.com/news.asp?newsID=12902>.
6. Y. Wang, Z. Shi, Y. Huang, Y. Ma, C. Wang, M. Chen and Y. Chen, *J. Phys. Chem. C*, 2009, **113**, 13103–13107.
7. J. Huang, B. G. Sumpter and V. Meunier, *Angew. Chem., Int. Ed.*, 2008, **47**, 520–524
8. J. Gamby, P. Taberna, P. Simon, J. Fauvarque and M. Chesneau, *J. Power Sources*, 2001, **101**, 109–116.
9. D. N. Futaba, K. Hata, T. Yamada, T. Hiraoka, Y. Hayamizu, Y. Kakudate, O. Tanaike, H. Hatori, M. Yumura and S. Iijima, *Nat. Mater.*, 2006, **5**, 987–994.
10. L. L. Zhang, R. Zhou and X. Zhao, *J. Mater. Chem.*, 2010, **20**, 5983–5992.
11. W. Tang, L. Liu, S. Tian, L. Li, Y. Yue, Y. Wu and K. Zhu, *Chem. Commun.*, 2011 **47**, 10058-10060.
12. F. Luan, G. Wang, Y. Ling, X. Lu, H. Wang, Y. Tong, X.X. Liu and Y. Li, *Nanoscale*, 2013, **5**, 7984-7990.
13. C.C. Hu, K.H. Chang, M.C. Lin and Y.T. Wu, *Nano Lett.*, 2006, **6**, 2690-2695.
14. X. Lu, G. Wang, T. Zhai, M. Yu, J. Gan, Y. Tong and Y. Li, *Nano Lett.*, 2012, **12**, 1690-1696.
15. X. Lu, T. Zhai, X. Zhang, Y. Shen, L. Yuan, B. Hu, L. Gong, J. Chen, Y. Gao, J. Zhou, Y. Tong and Z. L. Wang, *Adv. Mater.*, 2012, **24**, 938-944.

16. G. Yu, L. Hu, N. Liu, H. Wang, M. Vosgueritchian, Y. Yang, Y. Cui and Z. Bao, *Nano Lett.*, 2011, **11**, 4438-4442.
17. G. Yu, L. Hu, M. Vosgueritchian, H. Wang, X. Xie, J. R. McDonough, X. Cui, Y. Cui and Z. Bao, *Nano Lett.*, 2011, **11**, 2905-2911.
18. L. Wu, R. Li, J. Guo, C. Zhou, W. Zhang, C. Wang, Y. Huang, Y. Li and J. Liu, *AIP Adv.*, 2013, **3**, 082129.
19. L. Peng, X. Peng, B. Liu, C. Wu, Y. Xie and G. Yu, *Nano Lett.*, 2013, **13**, 2151-2157.
20. J. Feng, X. Sun, C. Wu, L. Peng, C. Lin, S. Hu, J. Yang and Y. Xie, *J. Am. Chem. Soc.*, 2011, **133**, 17832-17838.
21. J. Xie, X. Sun, N. Zhang, K. Xu, M. Zhou and Y. Xie, *Nano Energy*, 2013, **2**, 65-74.
22. J. Yan, Z. Fan, W. Sun, G. Ning, T. Wei, Q. Zhang, R. Zhang, L. Zhi and F. Wei, *Adv. Funct. Mater.*, 2012, **22**, 2632-2641.
23. V. Gupta, T. Kusahara, H. Toyama, S. Gupta and N. Miura, *Electrochem. Commun.*, 2012, **9**, 2315-2319.
24. H. Wang, Q. Hao, X. Yang, L. Lu and X. Wang, *Nanoscale* 2010, **2**, 2164-2170.
25. K. Jurewicz, S. Delpeux, V. Bertagna, F. Beguin and E. Frackowiak, *Chem. Phys. Lett.*, 2001, **347**, 36-40.
26. J. Tao, N. Liu, W. Ma, L. Ding, L. Li, J. Su and Y. Gao, *Sci. Rep.*, 2013, **3**, 2286.
27. A. Laforgue, P. Simon, C. Sarrazin, J. F. Fauvarque, *J. Power Sources*, 1999, **80**, 142-148.
28. Z. Yu, L. Tetard, L. Zhai and J. Thomas, *Energy Environ. Sci.*, 2015, **8**, 702-730.
29. C. Lin, J. A. Ritter and B. N. Popov, *J. Electrochem. Soc.*, 1999, **146**, 3155-3160.
30. K. Lota, A. Sierczynska and G. Lota, *Int. J. Electrochem.*, 2011, **2011**, 321473.
31. M. P. Yeager, D. Su, N. S. Marinkovic and X. Teng, *J. Electrochem. Soc.*, 2012, **159**, A1598-A1603.
32. Y.Z. Zheng, H.Y. Ding and M.L. Zhang, *Mater. Res. Bull.*, 2009, **44**, 403-407.
33. X. Du, C. Wang, M. Chen, Y. Jiao and J. Wang, *J. Phys. Chem. C*, 2009, **113**, 2643-2646.
34. L. Hu, W. Wang, J. Tu, J. Hou, H. Zhu and S. Jiao, *J. Mater. Chem. A*, 2013, **1**, 5136-5141.
35. C. Liu, F. Li, L. P. Ma and H. M. Cheng, *Adv. Mater.*, 2010, **22**, E28-E62.]

36. C. Portet, G. Yushin and Y. Gogotsi, *Carbon*, 2007, **45**, 2511-2518.
37. D. Pech, M. Brunet, H. Durou, P. Huang, V. Mochalin, Y. Gogotsi, P.L. Taberna and P. Simon, *Nat. Nanotechnol.*, 2010, **5**, 651–654
38. X. Lang, A. Hirata, T. Fujita and M. Chen, *Nat. Nanotechnol.*, 2011, **6**, 232–236
39. J. T. Mefford, W. G. Hardin, S. Dai, K. P. Johnston and K. J. Stevenson, *Nat. Mater.*, 2014, **13**, 726-732.
40. B. You, J. Yang, Y. Sun and Q. Su, *Chem. Commun.*, 2011, **47**, 12364-12366.
41. X. Tang, Z.-h. Liu, C. Zhang, Z. Yang and Z. Wang, *J. Power Sources*, 2009, 193, 939-943.
42. S.-W. Bian, Y.P. Zhao and C.Y. Xian, *Mater. Lett.*, 2013, 111,75-77.
43. C.Y. Cao, W. Guo, Z.M. Cui, W.G. Song and W. Cai, *J.Mater. Chem.*, 2011, **21**, 3204-3209.
44. W. Yu, X. Jiang, S. Ding and B. Q. Li, *J. Power Sources*, 2014, **256**, 440-448.
45. Z. Yang, F. Xu, W. Zhang, Z. Mei, B. Pei and X. Zhu, *J. Power Sources*, 2014, **246**, 24-31.
46. Y. Wang, A. Pan, Q. Zhu, Z. Nie, Y. Zhang, Y. Tang, S. Liang and G. Cao, *J. Power Sources*, 2014, **272**, 107-112.
47. X. Lai, J. Li, B. A. Korgel, Z. Dong, Z. Li, F. Su, J. Du and D.Wang, *Angew. Chem., Int. Ed.*, 2011, **50**, 2738-2741.
48. Z. Yang, F. Xu, W. Zhang, Z. Mei, B. Pei and X. Zhu, *J. Power Sources*, 2014, **246**, 24–31.
49. Z. Lei, Z. Chen and X. Zhao, *J. Phys. Chem. C*, 2010, **114**, 19867-19874.
50. Z. Lei, J. Zhang and X. Zhao, *J. Mater. Chem.*, 2012, **22**, 153–160.
51. L. Fan, L. Tang, H. Gong, Z. Yao and R. Guo, *J. Mater. Chem.*, 2012, **22**, 16376-16381.
52. Z. Lei, Z. Chen and X. Zhao, *J. Phys. Chem. C*, 2010, **114**, 19867-19874.
53. B. Duong, Z. Yu, P. Gangopadhyay, S. Seraphin, N. Peyghambarian and J. Thomas, *Adv. Mater. Interfaces*, 2014, 1, 1300014.
54. X. Lu, Y. Zeng, M. Yu, T. Zhai, C. Liang, S. Xie, M. S. Balogun and Y. Tong, *Adv. Mater.*, 2014, 26, 3148–3155.
55. G.Y. Zhao and H.L. Li, *Microporous Mesoporous Mater.*, 2008, **110**, 590–594.
56. Y.Y. Horng, Y.C. Lu, Y.K. Hsu, C.C. Chen, L.C. Chen and K.H. Chen, *J. Power Sources*, 2010, **195**, 4418–4422.

57. G. Q. Zhang, H. B. Wu, H. E. Hoster, M. B. Chan-Park and X. W. D. Lou, *Energy Environ. Sci.*, 2012, 5, 9453–9456.
58. H. Xia, J. Feng, H. Wang, M. O. Lai and L. Lu, *J. Power Sources*, 2010, 195, 4410–4413.
59. C.C. Hu, K.H. Chang, M.C. Lin and Y.T. Wu, *Nano Lett.*, 2006, 6, 2690–2695.
60. H. Pan, J. Y. Li and Y. P. Feng, *Nanoscale Res. Lett.*, 2010, 5, 654–668.
61. R. K. Sharma, A. Karakoti, S. Seal and L. Zhai, *J. Power Sources*, 2010, 195, 1256–1262.
62. C. Guan, J. Liu, C. Cheng, H. Li, X. Li, W. Zhou, H. Zhang and H. J. Fan, *Energy Environ. Sci.*, 2011, 4, 4496–4499.
63. K.S. Novoselov, A. K. Geim, S. V. Morozov, D. Jiang, Y. Zhang, S. V. Dubonos, I. V. Grigorieva and A. A. Firsov, *Science*, 2004, 306, 666–669.
64. Y. Zhu, S. Murali, M. D. Stoller, K. J. Ganesh, W. Cai, P. J. Ferreira, A. Pirkle, R.M. Wallace, K. A. Cychosz, M. Thommes, D. Su, E. A. Stach and R. S. Ruoff, *Science*, 2011, 332, 1537-1541.
65. M. D. Stoller, S. Park, Y. Zhu, J. and R. S. Ruoff, *Nano Lett.* 2008, 8, 3498-3502.
66. W. Lv, D.-M. Tang, Y.-B. He, C.H. You, Z.Q. Shi, X.-C. Chen, C.-M. Chen, P.X. Hou, C. Liu and Q.H. Yang, *ACS Nano*, 2009, 3, 3730–3736
67. Y. Zhu, M. D. Stoller, W. Cai, A. Velamakanni, R. D. Piner, D. Chen and R. S. Ruoff, *ACS Nano*, 2010, 4, 1227–1233]
68. M. F. ElKady, V. Strong, S. Dubin and R. B. Kaner, *Science*, 2012, 335, 1326-1330.
69. S. Shi, C. Xu, C. Yang, Y. Chen, J. Liu and F. Kang, *Sci. Rep.*, 2013, 3, 2598.
70. T. P. Gujar, V. R. Shinde, C. D. Lokhande, W.Y. Kim, K.D. Jung and O.S. Joo, *Electrochem. Commun.*, 2007, 9, 504-510.
71. L. Cao, S. Yang, W. Gao, Z. Liu, Y. Gong, L. Ma, G. Shi, S. Lei, Y. Zhang, S. Zhang, R. Vajtai and P. M. Ajayan, *Small*, 2013, 9, 2905-2910.
72. B. Lei, G. R. Li and X. P. Gao, *J. Mater. Chem. A*, 2014, 2, 3919-3925.
73. X. Wang, J. Ding, S. Yao, X. Wu, Q. Feng, Z. Wang and B. Geng, *J. Mater. Chem. A*, 2014, 2, 15958–15963.
74. J. M. Soon and K. P. Loh, *Electrochem. Solid-State Lett.*, 2007, 10, A250-A254.
75. J. Feng, X. Sun, C. Wu, L. Peng, C. Lin, S. Hu, J. Yang and Y. Xie, *J. Am. Chem. Soc.*, 2011, 133, 17832-17838.

76. M. R. Lukatskaya, O. Mashtalir, C. E. Ren, Y. Dall'Agnesse, P. Rozier, P. L. Taberna, M. Naguib, P. Simon, M. W. Barsoum and Y. Gogotsi, *Science*, 2013, **341**, 1502-1505.
77. M. Naguib, M. Kurtoglu, V. Presser, J. Lu, J. Niu, M. Heon, L. Hultman, Y. Gogotsi and M. W. Barsoum, *Adv. Mater.*, 2011, **23**, 4248-4253.
78. M. Kurtoglu, M. Naguib, Y. Gogotsi and M. W. Barsoum, *MRS Commun.*, 2012, **2**, 133-137.
79. M. Khazaei, M. Arai, T. Sasaki, C. Y. Chung, N. S. Venkataramanan, M. Estili, Y. Sakka and Y. Kawazoe, *Adv. Funct. Mater.*, 2013, **23**, 2185–2192.
80. H. Wang, Y. Liang, T. Mirfakhrai, Z. Chen, H. Casalongue and H. Dai, *Nano Res.*, 2011, **4**, 729-736.
81. J. Zhang, J. Jiang, H. Li and X. S. Zhao, *Energy Environ. Sci.*, 2011, **4**, 4009-4015.
82. J. Yan, Z. Fan, T. Wei, W. Qian, M. Zhang and F. Wei, *Carbon*, 2010, **48**, 3825-3833.
83. X. Dong, L. Wang, D. Wang, C. Li and J. Jin, *Langmuir*, 2012, **28**, 293-298.
84. J. Xie, X. Sun, N. Zhang, K. Xu, M. Zhou and Y. Xie, *Nano Energy*, 2013, **2**, 65-74.
85. Q. Qu, S. Yang and X. Feng, *Adv. Mater.*, 2011, **23**, 5574-5580
86. L. Fenghua, S. Jiangfeng, Y. Huafeng, G. Shiyu, Z. Qixian, H. Dongxue, I. Ari and N. Li, *Nanotechnology*, 2009, **20**, 455602.
87. Y. Zhang, H. Li, L. Pan, T. Lu and Z. Sun, *J. Electroanal. Chem.*, 2009, **634**, 68–71.
88. S. Ratha and C. S. Rout, *ACS Appl. Mater. Interfaces*, 2013, **5**, 11427–11433.
89. E. G. da Silveira Firmiano, A. C. Rabelo, C. J. Dalmaschio, A. N. Pinheiro, E. C. Pereira, W. H. Schreiner and E. R. Leite, *Adv. Energy Mater.*, 2014, **4**, 1301380
90. C. Wu, X. Lu, L. Peng, K. Xu, X. Peng, J. Huang, G. Yu and Y. Xie, *Nat. Commun.*, 2013, **4**, 2431.
91. W. Wang, S. Guo, I. Lee, K. Ahmed, J. Zhong, Z. Favors, F. Zaera, M. Ozkan and C. S. Ozkan, *Sci. Rep.*, 2014, **4**, 4452.
92. Y.M. Wang, X. Zhang, C.Y. Guo, Y.Q. Zhao, C.L. Xu and H.L. Li, *J. Mater. Chem. A*, 2013, **1**, 13290-13300.
93. T. Zhai, F. Wang, M. Yu, S. Xie, C. Liang, C. Li, F. Xiao, R. Tang, Q. Wu, X. Lu and Y. Tong, *Nanoscale*, 2013, **5**, 6790–6796.

94. M. J. Deng, P. J. Ho, C.-Z. Song, S.-A. Chen, J.-F. Lee, J.-M. Chen and K. T. Lu, *Energy Environ. Sci.*, 2013, **6**, 2178–2185.
95. X. H. Xia, J. P. Tu, Y. Q. Zhang, Y. J. Mai, X. L. Wang, C. D. Gu and X. B. Zhao, *J. Phys. Chem. C*, 2011, **115**, 22662–22668.
96. C. Zhou, Y. Zhang, Y. Li and J. Liu, *Nano Lett.*, 2013, **13**, 2078–2085.
97. Y. He, W. Chen, X. Li, Z. Zhang, J. Fu, C. Zhao and E. Xie, *ACS Nano*, 2013, **7**, 174–182.
98. Y. M. Wang, X. Zhang, C. Y. Guo, Y. Q. Zhao, C. L. Xu and H. L. Li, *J. Mater. Chem. A*, 2013, **1**, 13290–13300.
99. C. Zhou, Y. Zhang, Y. Li and J. Liu, *Nano Lett.*, 2013, **13**, 2078–2085
100. J. G. Speight, *Lange's handbook of chemistry*, MCGRAW-HILL, 16th edn, 2005.
101. A. G. Volkov, S. Paula and D. W. Deamer, *Bioelectrochem. Bioenerg.*, 1997, **42**, 153–160. E. R. Nightingale, *J. Phys. Chem.*, 1959, **63**, 1381–1387.
102. M. Y. Kiriukhin and K. D. Collins, *Biophys. Chem.*, 2002, **99**, 155–168.
103. M. Galin'ski, A. Lewandowski and I. Stepniak, *Electrochim. Acta*, 2006, **51**, 5567–5580.
104. A. Yu, V. Chabot and J. Zhang, *Electrochemical Supercapacitors for Energy Storage and Delivery: Fundamentals and Applications*, 2013.
105. K. Fic, G. Lota, M. Meller and E. Frackowiak, *Energy Environ. Sci.*, 2012, **5**, 5842–5850.
106. Q. Wang, J. Yan, Z. J. Fan, T. Wei, M. L. Zhang and X. Y. Jing, *J. Power Sources*, 2014, **247**, 197–203.
107. Z. Jin, X. D. Yan, Y. H. Yu and G. J. Zhao, *J. Mater. Chem. A*, 2014, **2**, 11706–11715.
108. L. F. Chen, Z. H. Huang, H. W. Liang, H. L. Gao and S. H. Yu, *Adv. Funct. Mater.*, 2014, **24**, 5104–5111.
109. L. J. Deng, J. F. Wang, G. Zhu, L. P. Kang, Z. P. Hao, Z. B. Lei, Z. P. Yang and Z. H. Liu, *J. Power Sources*, 2014, **248**, 407–415.
110. X. B. Liu, P. B. Shang, Y. B. Zhang, X. L. Wang, Z. M. Fan, B. X. Wang and Y. Y. Zheng, *J. Mater. Chem. A*, 2014, **2**, 15273–15278.
111. C. Feng, J. F. Zhang, Y. He, C. Zhong, W. B. Hu, L. Liu and Y. D. Deng, *ACS Nano*, 2015, **9**, 1730–1739.

112. I. I. Misnon, R. A. Aziz, N. K. M. Zain, B. Vidhyadharan, S. G. Krishnan and R. Jose, *Mater. Res. Bull.*, 2014, **57**, 221-230.
113. H. J. Wang, X. X. Sun, Z. H. Liu and Z. B. Lei, *Nanoscale*, 2014, **6**, 6577-6584.
114. B. S. Mao, Z. H. Wen, Z. Bo, J. B. Chang, X. K. Huang and J. H. Chen, *ACS Appl. Mater. Interfaces*, 2014, **6**, 9881-9889.
115. M. P. Bichat, E. Raymundo-Pinero and F. Beguin, *Carbon*, 2010, **48**, 4351-4361.
116. Q. Abbas, D. Pajak, E. Frackowiak and F. Beguin, *Electrochim. Acta*, 2014, **140**, 132-138.
117. C. Ramasamy, J. P. del Val and M. Anderson, *J. Power Sources*, 2014, **248**, 370-377.
118. S. Dhibar, P. Bhattacharya, G. Hatui, S. Sahoo and C. K. Das, *ACS Sustainable Chem. Eng.*, 2014, **2**, 1114-1127.
119. Y. Lin, X. Y. Wang, G. Qian and J. J. Watkins, *Chem. Mater.*, 2014, **26**, 2128-2137.
120. M. Sevilla and A. B. Fuertes, *ACS Nano*, 2014, **8**, 5069-5078.
121. R. Francke, D. Cericola, R. Kotz, D. Weingarth and S. R. Waldvogel, *Electrochim. Acta*, 2012, **62**, 372-380.
122. A. Brandt, P. Isken, A. Lex Balducci and A. Balducci, *J. Power Sources*, 2012, **204**, 213-219.
123. N. Jung, S. Kwon, D. Lee, D. M. Yoon, Y. M. Park, A. Benayad, J. Y. Choi and J. S. Park, *Adv. Mater.*, 2013, **25**, 6854-6858.
124. R. Vali, A. Laheear, A. Janes and E. Lust, *Electrochim. Acta*, 2014, **121**, 294-300.
125. D. Yigit, M. Gullu, T. Yumak and A. Sinag, *J. Mater. Chem. A*, 2014, **2**, 6512-6524.
126. S. D. Perera, M. Rudolph, R. G. Mariano, N. Nijem, J. P. Ferraris, Y. J. Chabal and K. J. Balkus, *Nano Energy*, 2013, **2**, 966-975.
127. E. Lim, H. Kim, C. Jo, J. Chun, K. Ku, S. Kim, H. I. Lee, I. S. Nam, S. Yoon, K. Kang and J. Lee, *ACS Nano*, 2014, **8**, 8968-8978.
128. X. D. Huang, B. Sun, S. Q. Chen and G. X. Wang, *Chem. Asian J.*, 2014, **9**, 206-211.
129. W. Li, T. Li, X. Ma, Y. Li, L. An and Z. Zhang, *RSC Adv.*, 2016, **6**, 12491-12496

130. C. C. Yang, S. T. Hsu and W. C. Chien, *J. Power Sources*, 2005, **152**, 303–310.
131. P. Sivaraman, A. Thakur, R. K. Kushwaha, D. Ratna and A. B. Samui, *Electrochem. Solid-State Lett.*, 2006, **9**, A435–A438.
132. J. Li and K. Lian, *Polymer*, 2016, **99**, 140–146.
133. Y. F. Huang, P. F. Wu, M. Q. Zhang, W. H. Ruan and E. P. Giannelis, *Electrochim. Acta*, 2014, **132**, 103–111.
134. J. K. Lee, Y. J. Lee, W. S. Chae and Y. M. Sung, *J. Electroceram.*, 2006, **17**, 941.
135. C. Ramasamy, J. Palma and M. Anderson, *J. Solid State Electrochem.*, 2014, **18**, 2903-2911.
136. A. Jain and S. K. Tripathi, *Ionics*, 2013, **19**, 549–557.
137. M. F. Hsueh, C. W. Huang, C. A. Wu, P. L. Kuo and H. Teng, *J. Phys. Chem. C*, 2013, **117**, 16751-16758.
138. X. Zhang, L. Wang, J. Peng, P. Cao, X. Cai, J. Li and M. Zhai, *Adv. Mater. Interfaces*, 2015, **2**, 1500267.
139. S. Ketabi, B. Decker and K. Lian, *Sol. State Ionics*, 2016, **298**, 73-79.
140. D. Kim, G. Lee, D. Kim and J. S. Ha, *ACS Appl. Mater. Interfaces*, 2015, **7**, 4608-4615
141. X. Liu, D. Wu, H. Wang and Q. Wang, *Adv. Mater.*, 2014, **26**, 4370.
142. F. Miao, C. Shao, X. Li, K. Wang and Y. Liu, *J. Mater. Chem. A*, 2016, **4**, 4180-4187.
143. E. Feng, G. Ma, K. Sun, F. Ran, H. Peng and Z. Lei, *New J. Chem.*, 2017, **41**, 1986–1992.
144. R. Wang, J. Lang, X. Yan, *Science China Chemistry*, 2014, **57**, 1570-1578.
145. C. Zhong, Y. Deng, W. Hu, J. Qiao, L. Zhang and J. Zhang, *Chem. Soc. Rev.*, 2015, **44**, 7484-7539.